

# An FGF23 missense mutation causes familial tumoral calcinosis with hyperphosphatemia

Anna Benet-Pagès<sup>1</sup>, Peter Orlik<sup>2</sup>, Tim M. Strom<sup>1,3,\*</sup> and Bettina Lorenz-Depiereux<sup>1</sup>

<sup>1</sup>Institute of Human Genetics, GSF National Research Center for Environment and Health, Ingolstädter Landstr. 1, 85764 Munich–Neuherberg, Germany, <sup>2</sup>Department of Pediatrics, Innsbruck Medical University, Anichstr. 35, 6020 Innsbruck, Austria and <sup>3</sup>Institute of Human Genetics, Klinikum rechts der Isar, Technical University, Ismaningerstr. 22, 81675 Munich, Germany

Received October 4, 2004; Revised November 19, 2004; Accepted November 26, 2004

GenBank accession nos<sup>†</sup>

**Familial tumoral calcinosis (FTC) is an autosomal recessive disorder characterized by ectopic calcifications and elevated serum phosphate levels. Recently, mutations in the *GALNT3* gene have been described to cause FTC. The FTC phenotype is regarded as the metabolic mirror image of hypophosphatemic conditions, where causal mutations are known in genes *FGF23* or *PHEX*. We investigated an individual with FTC who was negative for *GALNT3* mutations. Sequencing revealed a homozygous missense mutation in the *FGF23* gene (p.S71G) at an amino acid position which is conserved from fish to man. Wild-type FGF23 is secreted as intact protein and processed N-terminal and C-terminal fragments. Expression of the mutated protein in HEK293 cells showed that only the C-terminal fragment is secreted, whereas the intact protein is retained in the Golgi complex. In addition, determination of circulating FGF23 in the affected individual showed a marked increase in the C-terminal fragment. These results suggest that the FGF23 function is decreased by absent or extremely reduced secretion of intact FGF23. We conclude that FGF23 mutations in hypophosphatemic rickets and FTC have opposite effects on phosphate homeostasis.**

## INTRODUCTION

Familial tumoral calcinosis (FTC) [online mendelian inheritance in man (OMIM) 211900] is characterized by periarticular calcified masses often localized in the hip, elbow or shoulder (1). FTC is inherited in an autosomal recessive mode, but autosomal dominant inheritance has also been reported (2). The disease most commonly occurs in and usually appears before the second decade of life (1,3). FTC is associated with hyperphosphatemia and increased tubular phosphate reabsorption, but with normal serum levels of calcium and parathyroid hormone (4–6). Serum levels of 1,25-dihydroxyvitamin D may be normal or elevated (7).

Recently, biallelic mutations in the UDP-*N*-acetyl- $\alpha$ -D-galactosamine:polypeptide *N*-acetylgalactosaminyltransferase 3 (*GALNT3*) gene have been identified in two large families as a cause of FTC. *GALNT3* encodes a glycosyltransferase responsible for initiating mucin-type O-glycosylation. The findings suggested that defective post-translational

modification underlies this disorder. Furthermore, evidence for heterogeneity has been provided (8).

We investigated an individual with FTC where *GALNT3* mutations have been excluded. FTC seems to represent the metabolic mirror image of hypophosphatemic conditions, which are characterized by decreased serum phosphate levels, reduced tubular phosphate reabsorption and mostly rickets. One of these conditions is X-linked and is caused by loss of function mutations of the putative endopeptidase *PHEX* (9) (OMIM 307800). The other condition is caused by gain of function mutations of the putative circulating factor with phosphaturic activity, *FGF23* (10) (OMIM 193100) and a third condition, by over-expression of *FGF23* in tumor-induced osteomalacia (11,12). We therefore considered these genes candidates for FTC.

Sequence analysis of the *FGF23* gene showed a homozygous missense mutation (c.211A > G) in the affected individual resulting in a serine to glycine substitution (p.S71G). During secretion, wild-type FGF23 is processed

\*To whom correspondence should be addressed. Tel: +49 8931873296; Fax: +49 8931873297; Email: timstrom@gsf.de  
<sup>†</sup>AY753222 and AY753223.

by subtilisin-like proprotein convertases (SPC) into an N-terminal fragment which constitutes the  $\beta$ -barrel structure of the FGF protein family and a C-terminal fragment with no homologies to known proteins or motifs (11,13,14). We conclude from expression analysis and determination of FGF23 plasma levels that the novel missense mutation of FGF23 leads to decreased FGF23 function by nil or extremely reduced secretion of intact FGF23. This investigation also suggests FGF23 as a possible target of GALNT3.

## RESULTS

### Mutation analysis

We studied a 12-year-old boy who presented with typical symptoms of tumoral calcinosis. He had painful swellings at the left elbow and tibia (Supplementary Material, Figs S1 and S2). Repeated measurements showed elevated serum phosphate levels (Table 1) and increased tubular phosphate reabsorption. A dental panoramic radiograph revealed pulp stones at several teeth (Supplementary Material, Fig. S3). After exclusion of *GALNT3* mutations, sequencing identified a homozygous substitution (c.211A>G) at the last nucleotide of the first exon. The parents and one sister were heterozygous for the mutation, which was not found in 256 control alleles sequenced previously (Fig. 1) (10). This mutation most probably leads to a missense mutation substituting a serine by a glycine (p.S71G). The mutation is unlikely to cause aberrant splicing because it introduces a G which is most frequently used at this position and therefore increases the splice site consensus value as defined by Shapiro and Senapathy (15). Furthermore, it is possible to measure circulating FGF23 in the patient with antibodies directed against sequences C-terminal to the mutation.

In order to study whether the mutated serine is evolutionary conserved, we determined the *FGF23* sequence in other species by RT-PCR (*Tetraodon nigroviridis* and *Danio rerio*) or prediction from genomic sequence (*Gallus gallus*, *Xenopus tropicalis* and *Fugu rubripes*). Alignment of the sequences showed complete conservation of the serine residue from fish to mammals (Fig. 2). According to a model of FGF23 generated by the alignment of the protein sequence onto the superimposed crystal structure of FGFs (16), this serine is situated at the end of the loop between strands 3 and 4 of the FGF  $\beta$ -barrel structure.

### Expression in mammalian cells

We then investigated expression and processing of the mutated *FGF23* in HEK293 cells. Cells were stably transfected with *FGF23* carrying the mutation S71G (FGF23-S71G). Untransfected cells and cells transfected with native *FGF23* and the empty pcDNA3.1 vector were used as controls. Western blot analysis was performed on conditioned medium and total cellular lysate using polyclonal antibodies directed against peptides within the N-terminal (anti-FGF23<sub>48-67</sub>) (Fig. 3A) and the C-terminal fragments (anti-FGF23<sub>173-187</sub>) (Fig. 3B). In the conditioned medium of cells expressing native FGF23, we detected immunoreactive bands of ~30, 18 and 12 kDa, corresponding to secreted

**Table 1.** FGF23 plasma levels, phosphorus and calcium serum levels

Person	S71G mutation	FGF23 (RU/ml)	P (mmol/l)	Ca (mmol/l)
Controls	No	40/51/25/78/42		
Father	Heterozygous	45	1.16 (0.87–1.45)	2.37
Mother	Heterozygous	112	1.31 (0.87–1.45)	2.35
Sister	Heterozygous	59	1.36 (0.87–1.45)	2.41
Sister	No	92	1.19 (0.87–1.45)	2.45
Patient	Homozygous	1077	2.35–2.44 (1.05–1.75)	2.42–2.50

P, phosphorus; Ca, calcium.

Age dependent normal values for phosphorus are in parentheses.

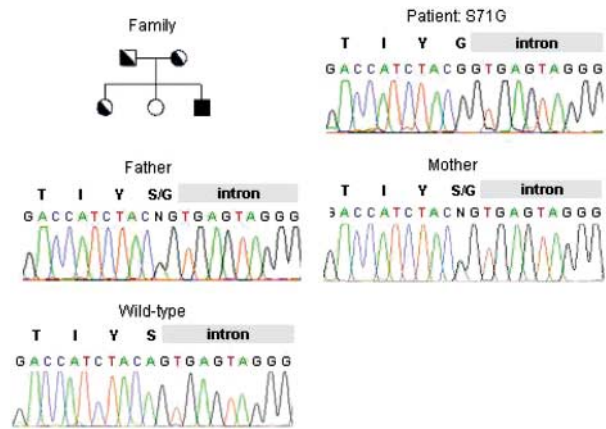


**Figure 1.** Mutation analysis. Segregation of the FGF23 c.211A>G transition (p.S71G) within an Austrian family and electropherograms of the family members. The affected individual is homozygous for the mutation; the parents and one sister are heterozygous.

intact FGF23<sub>25-251</sub>, N-terminal FGF23<sub>25-179</sub> and C-terminal FGF23<sub>180-251</sub>, respectively, whereas only after 1 day of exposure, a slight band corresponding to intact FGF23<sub>25-251</sub> was detected in the cell lysate. In contrast, conditioned medium of cells expressing mutant FGF23-S71G contained almost exclusively C-terminal FGF23<sub>180-251</sub> (12 kDa). Only very slight bands of intact FGF23<sub>25-251</sub> and N-terminal FGF23<sub>25-179</sub> were detected in seven of 10 and four of five experiments, respectively. Surprisingly, we detected a prominent band of ~25 kDa with both antibodies within the cell lysates. Other bands were not detected. Although this band migrated faster than FGF23<sub>25-251</sub> detected in the conditioned medium, it most probably represents intact FGF23<sub>25-251</sub> in another folding state. Alternatively, the difference in the apparent molecular weight may be caused by post-translational modifications or by digestions at the N- or C-terminal ends. We conclude that most of the mutant intact FGF23-S71G protein remained trapped within the cells, whereas only the C-terminal fragment was secreted.

### Subcellular localization of FGF23-S71G protein

As a consequence of mutation, proteins may be misfolded and degraded by the ubiquitin-proteasome system, may be

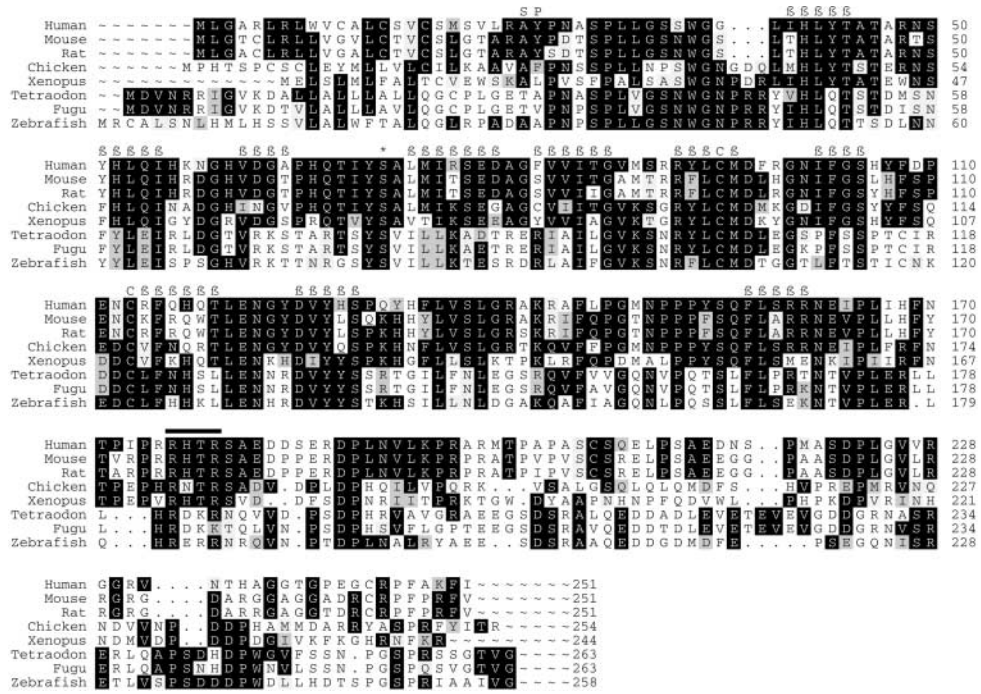


**Figure 2.** Amino acid sequence alignment of FGF23. Human (AAG09917), mouse (AAG09916) and rat (BAB84108) FGF23 were obtained from GenBank. *Gallus gallus* (Chicken), *X. tropicalis* (Xenopus), *F. rubripes* (Fugu), *T. nigroviridis* (Tetraodon) and *D. rerio* (Zebrafish) Fgf23 were predicted from the corresponding draft genome assemblies using tblastn and Genewise. *Danio rerio* and *T. nigroviridis* predictions were confirmed by RT-PCR. Of note, the *X. tropicalis* genome assembly (version 2) contained a second FGF23 homologous sequence (56% identity, 70% similarity) missing the proprotein convertase cleavage site (RXXR). Within the N-terminal  $\beta$ -barrel structure the conservation is high between all species. Within the peptide C-terminal fragment of the proprotein convertase cleavage site, the homology is divergent among classes and only highly conserved among mammals and fishes. The S71 site (asterisk) at which the S71G mutation occurred is conserved in all species investigated. The signal peptide cleavage site is indicated by 'SP', the cysteines presumably building a disulfide bond by 'C' (16), the  $\beta$ -strands by ' $\beta$ ', and the proprotein convertase cleavage site by a bold line. The alignment was generated with ClustalW and Prettybox.

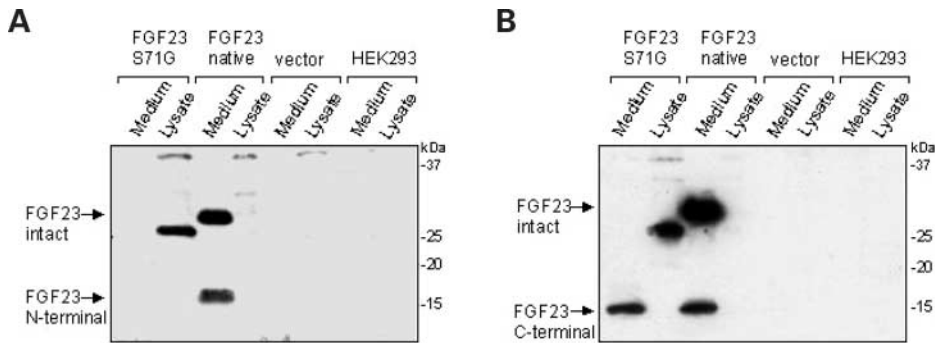


**Figure 3.** Expression of FGF23 and FGF23-S71G in HEK293 cells. Western blot analysis using anti-FGF23 polyclonal antibody against the N-terminal (anti-FGF23<sub>48-67</sub>) (A) and the C-terminal (anti-FGF23<sub>173-187</sub>) peptides (B) were performed in the conditioned medium and cell lysate of HEK293 cells expressing mutant FGF23-S71G, native FGF23, HEK293 cells stably transfected with empty pcDNA3.1 vector as well as untransfected HEK293 cells. Bands of 30, 18 and 12 kDa were detected in the conditioned medium of cells expressing native FGF23, whereas only a 12 kDa band was detected in the conditioned medium of cells expressing mutant FGF23-S71G. In addition, a 25 kDa band was detected in the cell lysate of cells expressing mutant FGF23-S71G protein. Controls were negative. Molecular mass markers are indicated to the right.

transported to lysosomes or may be retained within the endoplasmic reticulum or Golgi apparatus (17). To study the subcellular localization of the mutant protein, we generated constructs expressing the mutant and the wild-type protein for stable transfection in HEK293 cells. Primary antibodies against FGF23 (anti-FGF23<sub>148-163</sub>) and fluorochrome-labeled secondary antibodies were used to visualize the proteins. Antibodies and markers against different cellular

organelles were used for co-localization studies. FGF23-S71G, but not secreted wild-type protein, was detected within the cells (Fig. 4). Localization within the endoplasmic reticulum using an antibody against calnexin, within the lysosomes using an antibody against lysosome-associated membrane protein 1 and within the mitochondria using an antibody against a 60 kDa non-glycosylated protein component of mitochondria was excluded (data not shown).

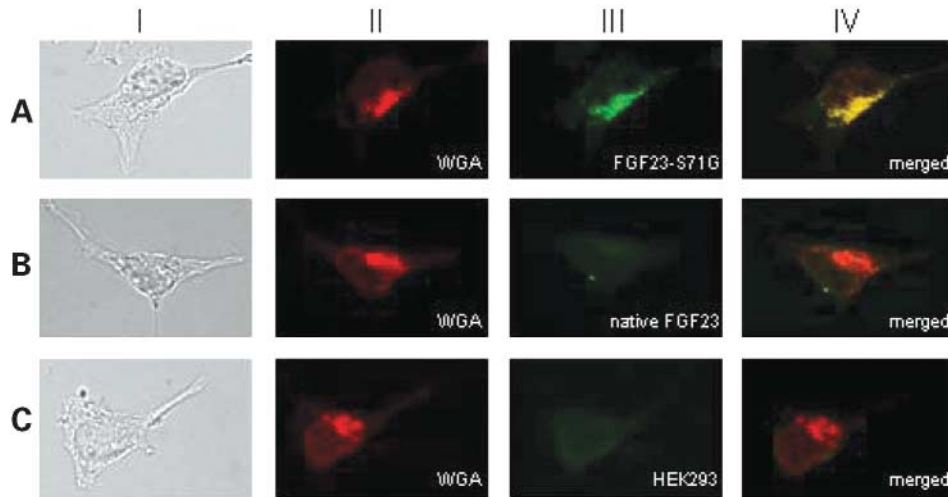


**Figure 4.** Subcellular localization of FGF23-S71G. Light microscopy images of HEK293 cells (column I) stably transfected with FGF23-S71G (A), native FGF23 (B) and untransfected HEK293 cells (C). Cells were stained with WGA Alexa Fluor 594 conjugate (red; column II) and anti-FGF23<sub>148–163</sub> antibody (green; column III). Merged images of the double-stained cells are shown in column IV. FGF23-S71G protein co-localized with the Golgi compartment specific WGA staining, whereas native FGF23 was not detected within the cells. HEK293 control cells showed no cross-reaction.

The green fluorescence of anti-FGF23<sub>148–163</sub> was localized to the polar perinuclear structure of the Golgi apparatus and perfectly co-localized with the red label of the Golgi marker Alexa Fluor 594 conjugate (Fig. 4A). Thus, at our levels of detection, FGF23-S71G is exclusively retained within the Golgi complex.

#### Serum levels of FGF23

To investigate the effect of mutant FGF23-S71G *in vivo*, we measured FGF23 plasma levels with an enzyme-linked immunosorbent assay (ELISA) detecting C-terminal and intact FGF23 in the patient, his parents, two sisters and five controls (Table 1). The FGF23 levels of normal controls ranged from 25 to 78 RU/ml (median 42 RU/ml), thus being within the normal range, which is <150 RU/ml for this assay (18). In addition, the parents and sisters of the patient showed plasma levels within the normal range (45, 112, 92 and 59 RU/ml). In contrast, the affected individual had a markedly elevated FGF23 level of 1077 RU/ml. Most probably, these elevated levels are the result of increased production and secretion of the C-terminal FGF23 fragment.

#### DISCUSSION

We have previously shown that gain of function mutations in the *FGF23* gene cause autosomal dominant hypophosphatemic rickets (ADHR) (10). Here, we report that the autosomal recessive hyperphosphatemic tumoral calcinosis (FTC), the metabolic mirror image of hypophosphatemia, can also be caused by a mutation in the *FGF23* gene. Sequence analysis of the *FGF23* gene in an affected individual revealed a homozygous missense mutation, encoding an S71G substitution, whereas non-affected family members were either heterozygous or homozygous for the wild-type allele

(Fig. 1). The heterozygous parents and one heterozygous sister showed no abnormalities in clinical and biochemical parameters, including serum FGF23 levels (Table 1), indicating that the expression of one *FGF23* allele can compensate the manifestation of FTC, which is consistent with *Fgf23*<sup>+/-</sup> mice (19). Our results are strengthened by the recent finding of an additional FGF23 mutation (S129F) causing tumoral calcinosis (20).

Interestingly, all *FGF23* mutations reported so far in ADHR (R176Q, R179Q, R179W) were located in the cleavage motif (RXXR) for an SPC responsible for processing of the protein (13,14,21). The new mutation in autosomal recessive FTC is located in the N-terminal  $\beta$ -barrel structure ~100 amino acids before the cleavage motif. The serine residue at position 71 is conserved among species, from fish to mammals (Fig. 2). According to structure modeling, it is situated at the end of the loop between strands 3 and 4 of the FGF  $\beta$ -barrel structure (16).

Cell culture experiments showed that intact FGF23-S71G is retained within the Golgi complex, whereas the C-terminal fragment is secreted (Figs 3 and 4). Retention in the Golgi complex has also been reported in other mutated proteins (22). We could not detect the N-terminal fragment either within the cell or in the conditioned medium. We conclude that this fragment is degraded. In order to study whether these *in vitro* experiments reflect the *in vivo* situation, we used a commercially available FGF23 sandwich ELISA that uses polyclonal antibodies against peptides within the C-terminal part of FGF23, thereby measuring intact FGF23 as well as the C-terminal fragment. We found markedly elevated levels in the affected individual. Most probably, these levels represent elevated concentrations of the C-terminal fragment as shown in the cell culture experiments. It has been shown that over-expression of full-length FGF23 in nude mice (23) and in tumor-induced osteomalacia (11,12) is associated with hypophosphatemia. It has also been

demonstrated that mutated FGF23 in ADHR (10,21) or when over-expressed causes hypophosphatemia. It is less well established whether N-terminal FGF23<sub>25–179</sub> or C-terminal FGF23<sub>180–251</sub> alone causes renal phosphate wasting. There is only a single report demonstrating that the administration of intact FGF23 to rodents caused renal phosphate wasting, whereas the administration of N-terminal FGF23<sub>25–179</sub> and C-terminal FGF23<sub>180–251</sub> did not (23). The results of this study exclude the possibility that the C-terminal fragment alone can cause phosphate wasting.

Elevated FGF23 levels have recently been reported in two families with FTC due to mutations in the *GALNT3* gene (8). The similarities between FTC caused by *GALNT3* and *FGF23* mutations, suggest that FGF23 may be a substrate of GALNT3. FGF23 has been described to be O-glycosylated (23). Nevertheless, it is unlikely that the serine substituted in FGF23-S71G is O-glycosylated. According to structure modeling, this serine is solvent inaccessible (16) and would sterically not allow O-glycosylation.

Hyperphosphatemia due to increased renal phosphate reabsorption and increased 1,25-dihydroxyvitamin D serum levels have also been found in *Fgf23* null-mice (19). However, this mouse model showed, in addition, severe bone tissue abnormalities, severe growth retardation and reduced life span possibly because of marked vascular calcification in the kidneys, impaired renal function and hypoglycemia. These differences between the mouse model and human FTC due to either *FGF23* or *GALNT3* mutations, can be explained either by residual function of FGF23 in humans or by inadequacy of the mouse model. A residual function may be explained by low levels of mutated intact FGF23, but a physiological function of the abundant C-terminal fragment cannot be excluded.

In conclusion, autosomal recessive hyperphosphatemic FTC is caused by a novel missense mutation in the *FGF23* gene. This report provides additional evidence that FGF23 is a physiological regulator of phosphate homeostasis. Further studies will be necessary to understand the role of FGF23 in the regulation of phosphate homeostasis.

## MATERIALS AND METHODS

### Family data and laboratory data

A 12-year-old boy from Austria presented with painful swellings at the left elbow and left tibia. Radiographs showed a calcified tumoral mass at the left elbow and signs of diaphysitis at the left tibia (Supplementary Material, Figs S1 and S2). Biopsy of the tumoral mass confirmed tumoral calcinosis by histologic analysis. Serum phosphate levels were elevated at repeated measurements (Table 1). Calcium (Table 1), parathormone [8.3–14.6 pg/ml (normal: 10–65 pg/ml)], 1,25-dihydroxyvitamin D [36.2–50.6 pg/ml (normal: 20–46 pg/ml)], AP [127–131 U/l (normal: 74–390 U/l)] and creatinine [0.44–0.54 mg/dl (normal: 0.3–1.0 mg/dl)] levels were normal. Tubular phosphate reabsorption (93–97%) and maximal tubular phosphate reabsorption (7.09–7.33 mg/dl) determined with the nomogram of Bijvoet were elevated (24). A dental panoramic radiograph revealed so-called pulp

stones at several teeth (Supplementary Material, Fig. S3). The parents and two sisters were unaffected.

### Mutation analysis

FGF23 exons were amplified with intronic primers and directly sequenced using a BigDye Cycle sequencing kit (Applied Biosystems, Foster City, CA, USA). Genomic DNA (~100 ng) was subjected to PCR amplification carried out in a 25 µl volume containing 1 × PCR MasterMix (Promega, Madison, WI, USA), 0.25 µM of each forward and reverse primer under the following cycle conditions: 95°C for 5 min, for 1 cycle; 95°C for 30 s, 60°C for 30 s and 72°C for 30 s, for 35 cycles; final extension 72°C for 5 min. Primer sequences are shown in Supplementary Material, Table S1.

### Mutagenesis and construction of expression vectors

The mutant FGF23-S71G cDNA (FGF23-S71G) was generated by site-directed mutagenesis (Stratagene, La Jolla, CA, USA) using a native FGF23 plasmid (FGF23/pBS) as template. The full-length FGF23 cDNA and the completely resequenced FGF23-S71G cDNA were subcloned for further experiments into the multiple cloning site of the mammalian expression vector pcDNA3.1 (Invitrogen, Carlsbad, CA, USA).

### Cell culture

Human embryonic kidney cells (HEK293) were maintained on RPMI 1640 (1 ×) with HEPES medium (PAA Laboratories, Cölbe, Germany), supplemented with 10% fetal calf serum (FCS), 50 IU/ml penicillin and 50 µg/ml streptomycin (Invitrogen). Cells were stably transfected with empty pcDNA3.1 vector (Invitrogen), native FGF23/pcDNA3.1 or FGF23-S71G/pcDNA3.1 plasmid using Effectene™ transfection reagent (QIAGEN, Hilden, Germany) and single clones were generated. Conditioned medium was collected after culturing the cells in serum-free medium for 24 h and it was concentrated 1:20 with Macrosep-omega 10 K concentrators (PALL Life Sciences, Dreieich, Germany) at 4°C. Protein concentrations were determined using the Bradford protein assay (Bio-Rad Laboratories, München, Germany). Cells were washed with PBS (PAA Laboratories), centrifuged for 5 min at 200g and cell pellets were resuspended in 500 µl lysis buffer (10 mM Tris-HCl/1% SDS).

### Western blot analysis

Protein samples (conditioned medium: 3 µg, cell lysate: 5–10 µg) were electrophoresed on 12% SDS-PAGE and electroblotted onto a BioTrace PVDF membrane (PALL Life Sciences). For the analysis of FGF23 protein, the membranes were incubated with 0.5 µg/ml anti-human FGF23 polyclonal antibody anti-FGF23<sub>48–67</sub> against N-terminal or anti-FGF23<sub>173–187</sub> against C-terminal peptides, described previously (13). Followed by detection with secondary HRP-conjugated goat anti-rabbit IgG antibody (Bio-Rad Laboratories), the signals were visualized with ECL plus system (Amersham Biosciences, Freiburg, Germany).

## Immunocytochemistry

HEK293 cells stably expressing mutant FGF23-S71G or native FGF23 protein and untransfected HEK293 cells as control, were grown on coated eight-chamber slides (Nunc, Wiesbaden, Germany) for 48 h. Cells were fixed in 4% paraformaldehyde for 15 min at room temperature, washed with PBS and permeabilized in PBS, 0.1% Igepal (Sigma, München, Germany) for 30 min followed by blocking with PBS, 3% BSA and 0.1% Igepal at 37°C. The primary antibody anti-FGF23<sub>148–163</sub> against an N-terminal peptide was diluted to a concentration of 2.5 µg/ml. Anti-calnexin (AF18) (Abcam, Cambridge, UK), anti-Lamp1 (LY1C6) (Abcam) antibodies, monoclonal antibody against human mitochondria (Chemicon, Temecula, CA, USA) and wheat germ agglutinin (WGA) Alexa Fluor 594 conjugate (Molecular Probes, Eugene, OR, USA) were diluted in the blocking solution as recommended by the manufacturers and incubated for 1 h at 37°C. Slides were washed in PBS, 0.1% Igepal three times for 10 min. The same incubation and washing procedures were used for the secondary antibodies anti-rabbit Alexa fluor 350 nm and anti-mouse Alexa fluor 568 nm (Invitrogen) diluted 1:1000 in the blocking solution. Preparations were visualized using an ApoTome Microscope (Zeiss, Jena, Germany).

## Circulating FGF23 levels

Plasma samples were isolated by centrifugation and stored at –70°C before biochemical analysis. FGF23 levels were measured using a commercial C-terminal two-site ELISA (Immutopics, San Clemente, CA, USA). The intra-assay CV for this assay is 5% and the inter-assay CV is 7.3%.

## SUPPLEMENTARY MATERIAL

Supplementary Material is available at HMG Online.

## ACKNOWLEDGEMENTS

We thank the patient and his family for participation in this study. This work was supported by a grant of the Deutsche Forschungsgemeinschaft (STR304/2-1).

## REFERENCES

- Palmer, P.E. (1966) Tumoural calcinosis. *Br. J. Radiol.*, **39**, 518–525.
- Lyles, K.W., Burkes, E.J., Ellis, G.J., Lucas, K.J., Dolan, E.A. and Drezner, M.K. (1985) Genetic transmission of tumoral calcinosis: autosomal dominant with variable clinical expressivity. *J. Clin. Endocrinol. Metab.*, **60**, 1093–1096.
- Prince, M.J., Schaeffer, P.C., Goldsmith, R.S. and Chausmer, A.B. (1982) Hyperphosphatemic tumoral calcinosis: association with elevation of serum 1,25-dihydroxycholecalciferol concentrations. *Ann. Intern. Med.*, **96**, 586–591.
- Lufkin, E.G., Kumar, R. and Heath, H., III (1983) Hyperphosphatemic tumoral calcinosis: effects of phosphate depletion on vitamin D metabolism, and of acute hypocalcemia on parathyroid hormone secretion and action. *J. Clin. Endocrinol. Metab.*, **56**, 1319–1322.
- Mitnick, P.D., Goldfarb, S., Slatopolsky, E., Lemann, J., Jr, Gray, R.W. and Agus, Z.S. (1980) Calcium and phosphate metabolism in tumoral calcinosis. *Ann. Intern. Med.*, **92**, 482–487.
- Lufkin, E.G., Wilson, D.M., Smith, L.H., Bill, N.J., DeLuca, H.F., Dousa, T.P. and Knox, F.G. (1980) Phosphorus excretion in tumoral calcinosis: response to parathyroid hormone and acetazolamide. *J. Clin. Endocrinol. Metab.*, **50**, 648–653.
- Slavin, R.E., Wen, J., Kumar, D. and Evans, E.B. (1993) Familial tumoral calcinosis. A clinical, histopathologic, and ultrastructural study with an analysis of its calcifying process and pathogenesis. *Am. J. Surg. Pathol.*, **17**, 788–802.
- Topaz, O., Shurman, D.L., Bergman, R., Indelman, M., Ratajczak, P., Mizrahi, M., Khamaysi, Z., Behar, D., Petronius, D., Friedman, V. *et al.* (2004) Mutations in GALNT3, encoding a protein involved in O-linked glycosylation, cause familial tumoral calcinosis. *Nat. Genet.*, **36**, 579–581.
- The HYP Consortium (1995) A gene (*PEX*) with homologies to endopeptidases is mutated in patients with X-linked hypophosphatemic rickets. *Nat. Genet.*, **11**, 130–136.
- The ADHR Consortium (2000) Autosomal dominant hypophosphatemic rickets is associated with mutations in FGF23. *Nat. Genet.*, **26**, 345–348.
- White, K.E., Jonsson, K.B., Carn, G., Hampson, G., Spector, T.D., Mannstadt, M., Lorenz-Depiereux, B., Miyauchi, A., Yang, I.M., Ljunggren, O. *et al.* (2001) The autosomal dominant hypophosphatemic rickets (*ADHR*) gene is a secreted polypeptide overexpressed by tumors that cause phosphate wasting. *J. Clin. Endocrinol. Metab.*, **86**, 497–500.
- Shimada, T., Mizutani, S., Muto, T., Yoneya, T., Hino, R., Takeda, S., Takeuchi, Y., Fujita, T., Fukumoto, S. and Yamashita, T. (2001) Cloning and characterization of FGF23 as a causative factor of tumor-induced osteomalacia. *Proc. Natl Acad. Sci. USA*, **98**, 6500–6505.
- Benet-Pages, A., Lorenz-Depiereux, B., Zischka, H., White, K.E., Econs, M.J. and Strom, T.M. (2004) FGF23 is processed by proprotein convertases but not by PHEX. *Bone*, **35**, 455–462.
- Liu, S., Guo, R., Simpson, L.G., Xiao, Z.S., Burnham, C.E. and Quarles, L.D. (2003) Regulation of fibroblastic growth factor 23 expression but not degradation by PHEX. *J. Biol. Chem.*, **278**, 37419–37426.
- Shapiro, M.B. and Senapathy, P. (1987) RNA splice junctions of different classes of eukaryotes: sequence statistics and functional implications in gene expression. *Nucleic Acids Res.*, **15**, 7155–7174.
- Harmer, N.J., Pellegrini, L., Chirgadze, D., Fernandez-Recio, J. and Blundell, T.L. (2004) The crystal structure of fibroblast growth factor (FGF) 19 reveals novel features of the FGF family and offers a structural basis for its unusual receptor affinity. *Biochemistry*, **43**, 629–640.
- Tsai, B., Ye, Y. and Rapoport, T.A. (2002) Retro-translocation of proteins from the endoplasmic reticulum into the cytosol. *Nat. Rev. Mol. Cell Biol.*, **3**, 246–255.
- Jonsson, K.B., Zahradnik, R., Larsson, T., White, K.E., Sugimoto, T., Imanishi, Y., Yamamoto, T., Hampson, G., Koshiyama, H., Ljunggren, O. *et al.* (2003) Fibroblast growth factor 23 in oncogenic osteomalacia and X-linked hypophosphatemia. *N. Engl. J. Med.*, **348**, 1656–1663.
- Shimada, T., Kakitani, M., Yamazaki, Y., Hasegawa, H., Takeuchi, Y., Fujita, T., Fukumoto, S., Tomizuka, K. and Yamashita, T. (2004) Targeted ablation of Fgf23 demonstrates an essential physiological role of FGF23 in phosphate and vitamin D metabolism. *J. Clin. Invest.*, **113**, 561–568.
- Araya, K., Fukumoto, S., Backenroth, R., Takeuchi, Y., Nakayama, K., Ito, N., Yamazaki, Y., Yamashita, T., Silver, J., Igarashi, T. *et al.* (2004) A mutation in FGF-23 gene enhances the processing of FGF-23 protein and causes tumoral calcinosis. *J. Bone Miner. Res.*, **19**, S41 (Abstr 1160).
- White, K.E., Carn, G., Lorenz-Depiereux, B., Benet-Pages, A., Strom, T.M. and Econs, M.J. (2001) Autosomal-dominant hypophosphatemic rickets (*ADHR*) mutations stabilize FGF-23. *Kidney Int.*, **60**, 2079–2086.
- Mulders, S.M., Bichet, D.G., Rijss, J.P., Kamsteeg, E.J., Arthus, M.F., Lonergan, M., Fujiwara, M., Morgan, K., Leijendekker, R., van der Sluijs, P. *et al.* (1998) An aquaporin-2 water channel mutant which causes autosomal dominant nephrogenic diabetes insipidus is retained in the Golgi complex. *J. Clin. Invest.*, **102**, 57–66.
- Shimada, T., Muto, T., Urakawa, I., Yoneya, T., Yamazaki, Y., Okawa, K., Takeuchi, Y., Fujita, T., Fukumoto, S. and Yamashita, T. (2002) Mutant FGF-23 responsible for autosomal dominant hypophosphatemic rickets is resistant to proteolytic cleavage and causes hypophosphatemia *in vivo*. *Endocrinology*, **143**, 3179–3182.
- Walton, R.J. and Bijvoet, O.L. (1975) Nomogram for derivation of renal threshold phosphate concentration. *Lancet*, **2**, 309–310.